YALE
PEABODY
MUSEUM

JOURNAL OF MARINE RESEARCH

The *Journal of Marine Research,* one of the oldest journals in American marine science, published important peer-reviewed original research on a broad array of topics in physical, biological, and chemical oceanography vital to the academic oceanographic community in the long and rich tradition of the Sears Foundation for Marine Research at Yale University.

An archive of all issues from 1937 to 2021 (Volume 1–79) are available through EliScholar, a digital platform for scholarly publishing provided by Yale University Library at https://elischolar.library.yale.edu/.

Requests for permission to clear rights for use of this content should be directed to the authors, their estates, or other representatives. The *Journal of Marine Research* has no contact information beyond the affiliations listed in the published articles. We ask that you provide attribution to the *Journal of Marine Research.*

The COBLAMED satellite buoy experiment: A measure of small scale horizontal variability in the upper layer

by David H. Shonting[1] and Alan T. Massey[1]

ABSTRACT

A satellite buoy experiment, which was conducted during COBLAMED in the Western Mediterranean, consisted of a thermistor buoy tethered to an identical moored buoy in a mean current at separation distances of 100 and 400 m in order to observe the dependence of small scale variability upon internal waves and advection and to register time and depth variability of horizontal coherence. The two 18-hour records showed distinct warm and cold pulses which traversed the separations with the mean current and preserved their shapes. The simultaneous records displayed very similar highly correlated wave-like fluctuations attributable to low frequency, long wavelength internal waves. Cross-spectral half coherence values ranged from 1-5 cph and 0.5-1.7 cph for the 100 and 400 m separations, respectively, with the coherences displaying a strong dependence on the local temperature (density) gradient. The observed temperature variability was attributable to (1) diurnal surface heating, (2) meso scale quasi-random thermal events being advected past the buoys with the mean current and (3) low frequency, long wavelength internal waves propagating much faster than the advection speeds. The results indicate that use of a tethered buoy system appears a viable technique to study horizontal scales of variability.

1. Introduction

It is becoming increasingly evident that the mechanisms related to energy and heat fluxes in the upper ocean are associated with meteorological events that are often intermittently distributed both in space and time (Mollo-Christensen, 1970); a quality which at the outset renders meaningful measurements difficult. In order to evaluate the important scales over which such energy fluxes occur, precise observations are required of variables such as temperature and current for determination of their spatial and temporal correlations and spectral coherence. Horizontal correlation and coherence of temperature and currents are more difficult to measure than their vertical counterparts because the latter observations require only sensors on a single taut mooring, to register time variability with depth, whereas multiple (and costly) arrays of fixed moorings or elaborate ship-towed systems are needed to record horizontal variability. Furthermore, in the presence of normally strong vertical

---

1. Naval Underwater Systems Center, Newport Laboratory, Newport, Rhode Island, 02840, U.S.A.

stratification, horizontal correlation and coherence estimates from fixed sensors are easily biased by small depth errors in ostensibly "identical depths." Similar control problems arise with sensors which are towed at "constant depths."

Estimates of spatial correlation and cross-spectral coherence of currents made at fixed positions in the open ocean (e.g., Webster, 1968 and Seidler, 1971) show that vertical coherence falls off much faster at higher frequencies than do horizontal coherences. Current observations in Rhode Island Sound made at identical shallow depths but with a 1.0-1.5 km separation were much more highly correlated than were data from instruments on the same moorings vertically separated 20 m through the summer thermocline (Shonting, 1969). These results are ascribed to the stable vertical stratification which decouples the layers thereby inhibiting vertical transfer of momentum and heat, whereas a relatively freer interchange (and hence higher correlation) occurs laterally across the much weaker horizontal gradients.

Schott (1971) measured horizontal coherence of currents in the North Sea from an array of buoys with separations of 2.3 to 4.5 km. His results exhibited strong tidal and inertial effects. The coherences were high for 2.5 km horizontal separation at tidal frequencies but decreased rapidly above a frequency of 0.2 cycles per hour (cph).

Zalkan (1970) made observations of isotherm oscillations from sensors mounted on booms from the "Flip" platform while it was drifting in the deep sea off Baja, California. Coherences over 30 m separation distances displayed a strong decrease above 3-6 cph. Pinkel (1975) obtained horizontal coherences from temperature data at depths of 60-240 m from "Flip" using 40 m horizontal booms in an attempt to observe anisotropy in an internal wave field. Pinkel infers that a 40 m separation was too small to resolve directional or anisotropic properties of the internal waves below the mixed layer.

Probably the most comprehensive spatial observations thus far obtained are from the Internal Wave Experiment (IWEX) described by Briscoe (1975). Current and temperature sensors placed in a tri-moor located 700 km SW of Bermuda from depths of 600-2050 m provided coherences from horizontal separations ranging from 14-1600 m. Samples of temperature cross-spectra where the buoyancy frequency ranged from 0.66-2.54 cph suggested strong horizontal isotropy. Coherence of temperature dropped steadily with increased separation. Preliminary results show that the product of the half coherence frequency (in cph) and the separation (in m) equals 330 m cph; this suggests that the coherence was independent of depth or buoyancy frequency. It is clear that more experimental data are needed to fill in the picture of ocean variability, especially from scales from 10 to 1000 m, a distance difficult to instrument precisely, particularly in the upper layers where strong perturbations occur with the rapidly changing wind, wave and thermal conditions.

This paper presents results of an experiment conducted in the western Mediterranean to provide a unique measure of horizontal correlations and variability of
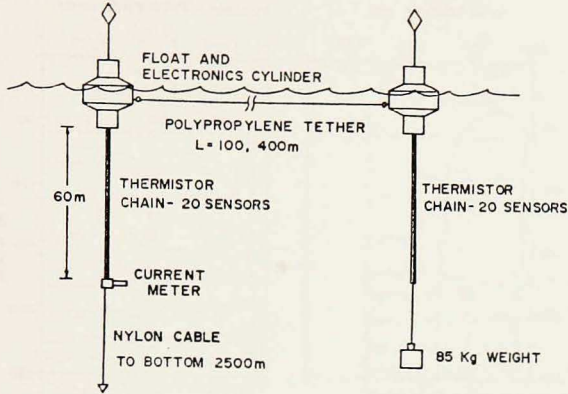
Figure 1. Configuration of the satellite buoy experiment.

temperature structure in the upper ocean over a depth range from the surface to 60 m in 2500 m deep water, separated at horizontal distances of 100 and 400 m. This experiment was part of a larger scale observational program, COBLAMED '69 (Shonting, 1974), which utilized moored buoys and ships in the Gulf of Lions to record synoptically the response of the upper layer temperature and current to the surface wind stress.

2. Instrumentation and observations

The horizontal correlation measurements were made using a pair of buoys (Fig. 1), each supporting a self-recording thermistor cable system containing 20 sensors spaced at depths from 0.5 m to 60 m (for instrumentation details, see Shonting *et al.*, 1972). Buoy Delta was taut moored in 2500 m of water, the satellite buoy Echo was tethered to Delta by a polypropylene (buoyant) cable at separation distances L = 100, 400 m. For stability, an 85 kg weight was fastened at the bottom of the Echo thermistor array.

The currents observed in the area, which normally ranged from 5-30 cm/sec (Shonting, 1974), kept the buoy Echo at a distance of the tether length. Delta thus served as a reference used to compare continuously the temperature structure registered at the identical depths at satellite buoy Echo. This configuration also allowed a measure of advection of any gross variability which should occur along the mean current stream line into which the buoys were aligned.

Temperatures were recorded on each system every three minutes, being logged on an fm magnetic tape storage unit housed in the surface pressure case (Fig. 1). The sensors were potted in epoxy resin giving them a response time of about 4 min. This eliminated aliasing caused by the systems' oscillating (from float response to surface waves) through isotherms at frequencies of 0.14-0.3 Hz.
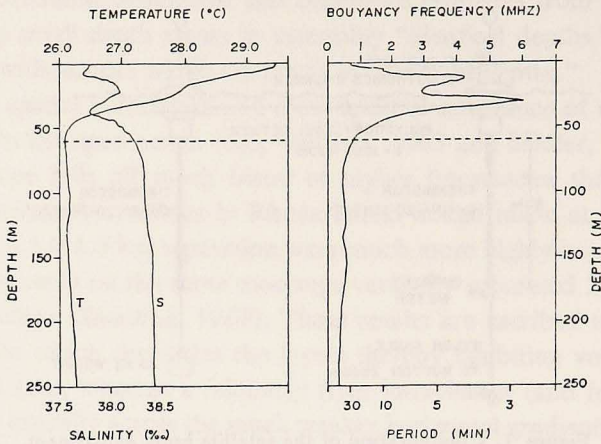
Figure 2. Typical temperature-salinity profiles taken near Buoy Delta at 1620 GMT on 12 Sep 69 (left curves). At right, the resulting buoyancy frequency profile.

The timing accuracy of the synchronized clocks in each buoy minimized the uncertainty in the simultaneity of the sampling time to within one sampling interval (182 sec). Pairs of simultaneous 18 hour records were obtained for the 100 and 400 m horizontal separations.

3. Results

The intense seasonal thermocline in the COBLAMED area is shown by the temperature profile made near Buoy Delta using a Plessey STD system (Fig. 2). The temperature and salinity conditions shown are typical for the late summer and fall for the Gulf of Lions; the strong stratification keeping the mixing and high variability to the upper 50-70 m. The high stability of the upper layer is underscored by the double peaked buoyancy frequency profile calculated from the STD data.

Temperature traces for the simultaneous buoy records for thermistors in the upper depths are displayed in Figure 3. The vertical bars separate portions of the records made with the 100 and 400 m horizontal tether. The strong similarity of the Delta and Echo records indicates that the tether distances and sampling intervals were sufficiently small for resolving variability which is largely preserved over the time and space scales of the sampling.

Before reaching conclusions about the data, it was necessary to assess any possible differences in the depths of the sensors on each array; otherwise, strong biasing could occur in the estimates of horizontal variability in the presence of observed large vertical temperature gradients (Fig. 2). Vertical displacements of sensors could come about in two ways: (1) tilting of arrays off-vertical because of current or wind drag, which would likely act differently in each array, and (2) errors in the
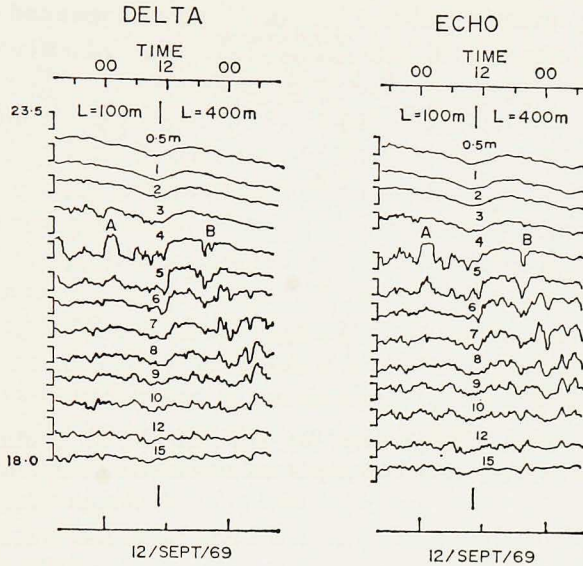
Figure 3. Temperature records for the upper 15 m depth simultaneously recorded at the two buoys.

placement of the thermistors on the cable or unequal freeboard of the buoys in their equilibrium positions. The vertical displacement of the sensors due to linear tilting of the array would vary as $l \, (1 - \cos \Theta)$ where l is the distance of the sensor from the surface buoy and Θ is the angle subtended by the array with the vertical. A thermistor which is displaced δz (z positive upward) will experience a change in temperature.

$$\delta T = (\partial T(z)/\partial z) \, \delta z \tag{1}$$

where $\partial \bar{T}(z)/\partial z$ is the local mean vertical temperature gradient, at depth z.

If each thermistor system undergoes a vertical displacement δz then, denoting subscripts D and E for each buoy, the resulting temperature difference is

$$\Delta T = \left(\frac{\partial T}{\partial z}\right)_D (\delta z)_D - \left(\frac{\partial T}{\partial z}\right)_E (\delta z)_E \tag{2}$$

The $(\delta z)_D$ and $(\delta z)_E$ will be constant with depth for a total displacement of the thermistor array or from (1) will increase linearly with l for a tilted array whose support cable has a negligible catenary. For buoy separations of 100 and 400 m, we use the approximation

$$\frac{\partial T}{\partial z} \cong \frac{1}{2}\left[\left(\frac{\partial T}{\partial z}\right)_D + \left(\frac{\partial T}{\partial z}\right)_E \right]$$
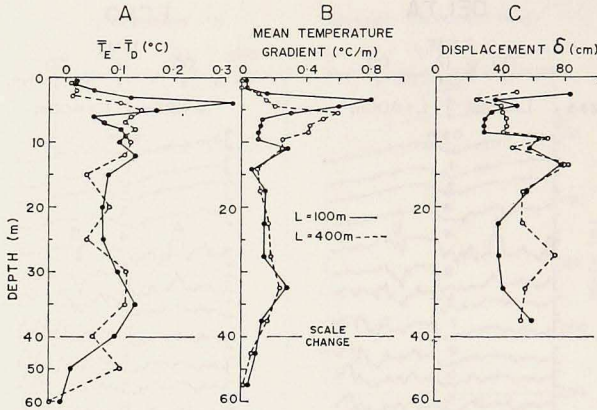
Figure 4. Difference in mean temperatures (A); mean temperature gradients (B); estimated mean displacements of buoy Echo (with respect to Delta) at each sensor depth (C).

and thus

$$\Delta T(z) = \frac{\partial T(z)}{\partial z} \ [(\delta z)_D - (\delta z)_E] = \delta \frac{\partial T}{\partial z} \tag{3}$$

where we define δ as the net depth difference between respective sensors.

Estimates were made of δ for both the 100 m and 400 m experiments using the data plotted in Figure 4. Curves "A" show the differences between the mean temperatures at each depth for each experiment. Note that at all depths Echo temperatures were warmer than those of Delta (i.e., all positive differences). The curves "B" are the vertical temperature gradients estimated by taking the mean values at each depth, calculating the corresponding gradients between vertical consecutive pairs, and then averaging Delta and Echo values at each depth. These curves are in effect a first order approximation of the buoyancy frequency which ranged from 2 cph (at 50 m) to 25 cph (at 4 m); equivalent to 0.8° C/m in the separation L = 100 m curve. Two temperature gradient maximums, the upper at 5-7 m, the lower at 30-35 m, persist throughout the measurements; their presence is consistently reflected in the various statistics discussed further.

The mean gradient profiles indicate the strong surface mixing of 12-13 September. During the two 18-hour consecutive recording periods, the wind increased continuously from 5 to 18 m/sec over the period of the 100 and 400 m observations; thus, a higher degree of mixing is exhibited for the 400 m separation experiment than for the 100 m experiment. However, below 12 m the temperature structure remained about the same.

These profiles closely follow the mean temperature differences, and furthermore, the values of δ (Fig. 4C) appear to be approximately independent of depth. Values of δ are not shown for $z < 4$ m or $z > 40$ m since in these regions $\partial T/\partial z$ is small

and relation (3) becomes unstable. It is noted that in general the plots of δ except for 27.5 m are similar for both data sets even though the dynamic drag was likely much higher during the L = 400 m experiment due to high winds and sea states.

Conclusions from these results are: (1) Differential tilting of the arrays was negligible since δ does not increase linearly or otherwise with depth and (2) Echo array was in fact actually riding shallower than array Delta by an amount (estimated between depths of 4 and 40 m) of 45-50 cm. The discrepancies occurring in the values of δ for both experiments may indicate the errors made in the original placement of some of the sensors, e.g., especially between 10 and 15 m depths. Moreover, a mean depth difference between buoys Delta and Echo is understandable since Delta was taut moored to the bottom with 6-8 times the tension of Echo. This would force the Delta surface float to remain nearer the wave troughs whereas Echo would tend to ride the troughs and crests, giving it a higher mean level. The surface waves occurring during the measurements where winds ranged from 5-18 m/sec had observed average amplitudes of at least 40-60 cm.

The temperature curves at 0.5 and 1.0 m vertical separations (Fig. 3) show strong identity between adjacent traces thus, it is assumed that the 30-50 cm mean displacement between Delta-Echo sensors will cause negligible errors in the cross statistics discussed in the foregoing analysis. (By appropriate interpolation temperatures could be adjusted to assimilate zero δ values for perhaps more precise intercomparison).

Returning to the Delta/Echo records (Fig. 3), aside from their strong similarity, they portray a variety of phenomena, namely:

1. A diurnal heat wave oscillation detectable down to 7-8 m.
2. A gradual cooling of the upper 3-4 m layer during the strong wind mixing from 11-12 September.
3. Periodic oscillations occurring below 3 m up to 1.5 m amplitudes which are in-phase over several meters in the vertical suggesting internal wave activity of periods from 0.5-6 hours. The higher frequency part of these oscillations (from 0.5-1 hour periods) appears progressively smoothed with both time and depth (from 3-5m). This phenomena, which was registered at all of the COBLAMED buoy systems, is associated with the intense wind mixing and is discussed in detail by Shonting and Goodman (1978).
4. Sporadic aperiodic warm and cold pulses (e.g., A and B); these occur on both records suggesting horizontal advection of small structure with a conserved signature detected by each array.

The strong similarities and statistical stability of the records at Delta and Echo are emphasized by the profiles of variance (Fig. 5) and correlation coefficients (Fig. 6). The individual 100 and 400 m separation experiments demonstrate remarkable respective similarity whereby maximum values of fluctuations correspond to the region of strongest vertical gradient (Fig. 4B).
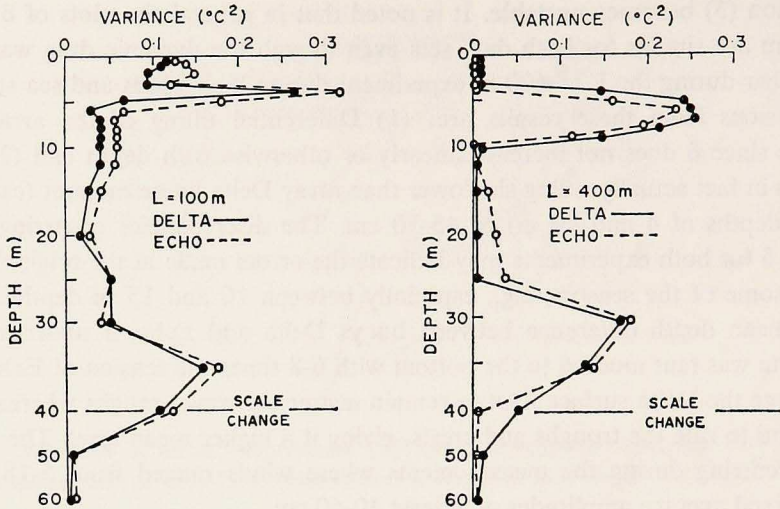
Figure 5. The variance of Delta and Echo temperatures with depth for the 100 and 400 m separation records.

The linear correlation coefficient for both separations approaches unity at the surface, reflecting the diurnal (low frequency) fluctuations which are uniform, i.e., in phase for the whole COBLAMED area. The other maximum occurs at 30-40 m where the maximum gradient occurs (Fig. 4B) suggesting that here scales of variability (e.g., internal wavelengths) are much larger than the sensor separations and larger than the dominant scales of variability existing between 5 and 30 m.

4. Measure of horizontal advection

The configuration and manner of data recording of the Delta-Echo systems allows detection of horizontal variability as it is advected by the buoy pair in the surface layer since the buoy Echo tends to align itself in a streamline of the flow down current from Delta. Furthermore, three minute sensor sampling intervals are smaller than the advective transit time of a water parcel moving from Delta to Echo (which for L = 100 m and for the highest recorded current speed of 32 cm/sec is over 310 sec).

The records (Fig. 3) show sporadic pulses and wiggles peculiar to both traces which appear to be associated with distinct patches of warm or cold water. Superposition of the record pairs with time shows a consistent phase difference; these events always occur first at Delta, then at Echo. For example, the leading edge of the warm pulse A (Fig. 3) at Delta precedes Echo by about 8 minutes; for the L = 100 m gives an equivalent advection speed of about 21 cm/sec. For event B, the lag between Delta and Echo is about 25 minutes equivalent to 27 cm/sec for L =
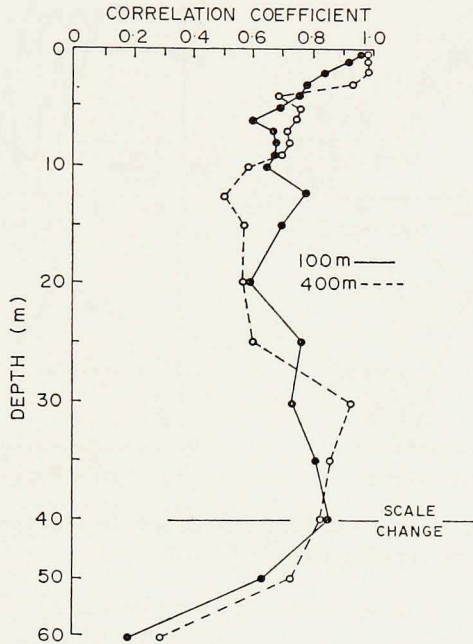
Figure 6. The linear correlation coefficients between Delta and Echo records for the 100 and 400 m separations.

400 m. These estimated advection speeds agree well with mean currents observed in the general COBLAMED area 7.5 km distant (Shonting, 1974).

Estimates of advection speed made by comparing leading (or trailing) edges of pulses are crude, since the signal pairs can differ in their shapes and slopes. For a more quantitative examination of advection effects, two events (Fig. 7—upper curves) were studied, consisting of a 45 min. warm pulse at 35 m for L = 100 m and a 60 min. cold pulse at 4 m for L = 400 m. The leading edge of Delta record leads Echo in both cases. The linear correlation coefficient was estimated as a function of time lags in which the Echo series was shifted by increments of the sampling interval of $\Delta t = 182$ seconds (producing, in effect, the auto correlation function over several lags). The results (Fig. 7—lower curves) indicate an initial correlation of 0.6, which peaks at 6 minutes, whereas for 400 m separation, a near zero initial correlation peaks at 21.3 minutes. These values provide advection speeds of 27 and 31 cm/sec, again similar to observed values. In comparison, phase speeds calculated for the first mode internal waves using the local buoyancy profile (similar to that in Fig. 2) are, for one and three cph, 88 and 28 cm/sec respectively.

We note in Figure 7 that the correlations (at zero lag) are 0.58 and −0.10, respectively, values determined from 40 and 45 data points. However, Figure 6
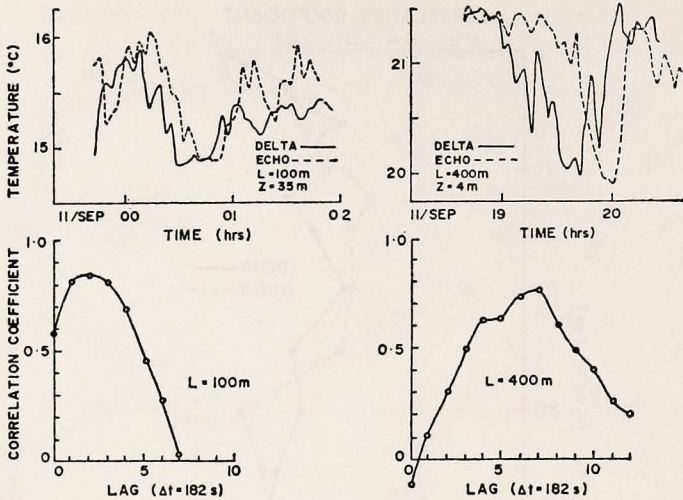
Figure 7. Abrupt changes in Delta and Echo records and the corresponding covariance function evaluated over several sampling intervals (Lags).

shows correlation values of 0.81 and 0.68 for the 35 m (L = 100 m) and 5 m (L = 400 m), respectively. It is suggested that the high average correlation between records must be associated with persistent wavelike phenomena; e.g., diurnal heating at the surface (totally correlated in space and time) or from internal waves having wavelengths much larger than L. If, on the other hand, the variability were caused entirely of advected events of abrupt or discrete parcels of smaller or larger horizontal scale than the buoy separations, correlations (at zero lag) would be low. From Figure 7 the time interval for the passage of both cold pulses is about one hour. Using the estimated current speeds, the horizontal dimensions of the two cold pulse events spanning the approximate leading and trailing edges is inferred to be about 1 km.

5. Spectra and coherence

Representative auto spectra of temperature for several depths are given in Figure 8, having approximately 15 degrees of freedom (the 90% confidence limit bar is shown). The records span the entire 39 hour period bracketing both sets of Delta-Echo observations. A negative 5/3 slope is presented for comparison. Above 0.5 cph, records at 5, 10, and 35 m display high energy which roughly corresponds to the depths of strong density gradients (Fig. 4B) and of large temperature variance (Fig. 5). Conversely, the fall-off of energy above 0.5 cph for the 1 and 60 m curves is associated with weak vertical gradients. Below 0.5 cph, sensors at 1 and 5 m record strong diurnal oscillations; the high energy density at 35 m may be related
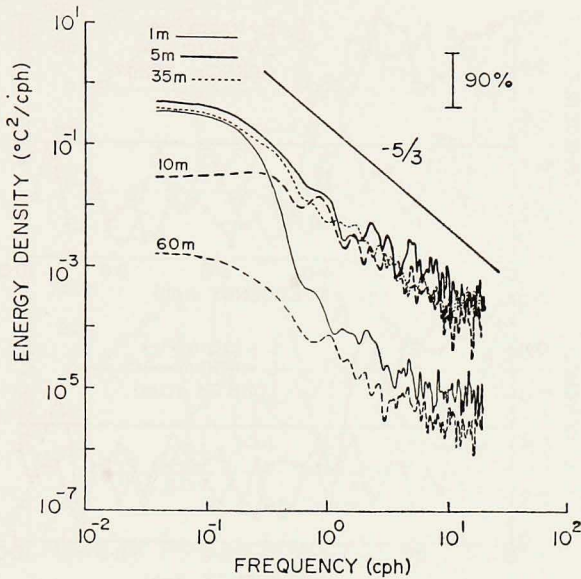
Figure 8. Auto-spectra for Delta temperature records at several depths. The 90% confidence limit bar is shown for 15 degrees of freedom.

to the observed strong 17.6 h inertial oscillations (Shonting, 1974) although no peak is resolved on the 40 hour record.

The relationship between the temperature signals at Delta and Echo depends upon the space and time scales of the local temperature variability in relation to the separation L and the buoy-to-buoy transit time $L/\bar{U}$ where $\bar{U}$ is the local mean advection speed. Visually, the simultaneous records both for L = 100 and 400 m are dramatically similar; a fact verified by the high positive correlations (Fig. 6). The correlation coefficient, however, is determined largely by the correspondence of the linear and lower frequency components of the fluctuations. The cross-spectral coherence estimated between the record pairs made at identical depths provides a more quantitative picture of the scales of variability since it registers the degree of correlation as a function of frequency. Thus, one can compare both wave-like phenomena (highly stationary) and advective changes (weakly stationary).

Coherences were estimated for the data pairs for each separation distance (i.e., L = 100, 400 m). Examples of the coherence at 35 and 40 m depths (in a region of the strongest temperature gradient) are shown in Figure 9. The estimates were made using 397 data pairs with 40 spectral bands equivalent to 20 degrees of freedom (Kinsman, 1965). The horizontal broken line is the level at which 90% of the estimated values would fall for a null hypothesis were there a zero coherence between the Delta and Echo records (Granger and Hatanaka, 1964).
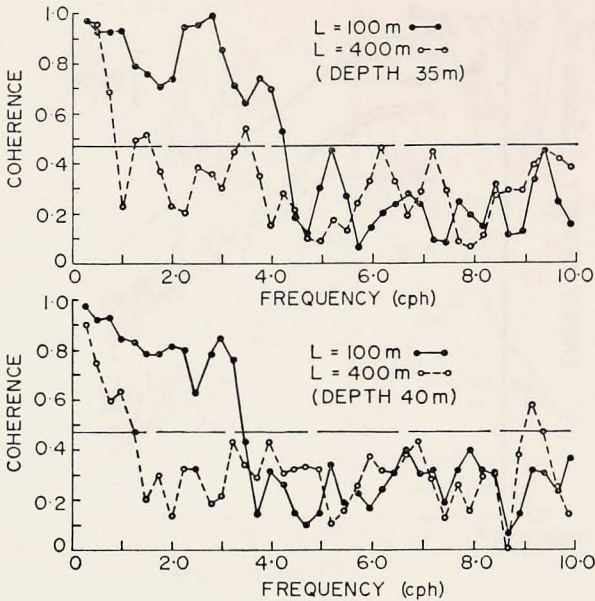
Figure 9. Cross-spectral coherence between records of Delta and Echo for the 100 and 400 m separations at 35 and 40 m depths in the region of the strongest temperature gradient.

The $L = 100$ m and 400 m plots show striking similarity in shape, respectively, for the 35 and 40 m depths, suggesting very stable statistics not common for coherence estimates. The $L = 400$ m coherences clearly fall off much faster with increasing frequency than do the $L = 100$ m estimates. The half coherence frequency commonly designated by $f\frac{1}{2}$ (Webster, 1972) for the 35 and 40 m depths is roughly 1.2 cph for $L = 400$ m and 4 cph for $L = 100$ m. If these equivalent periods $f\frac{1}{2}$ are multiplied by a $\bar{U}$ of 25 cm/sec, the equivalent cutoff scales become 750 and 225 m, respectively.

The phase relations for sensors at 35 and 40 m for each separation (Fig. 10) display both interesting similarities and differences. First, for low frequencies (up to 0.5 cph) values are near zero; this agrees with IWEX data for similar distances (Briscoe, 1975) and is plausible since for low frequencies scales (including inertial motions at 0.064 cph) would be much larger than the sensor separations. Above 0.5 cph the 100 m separation phase monotonically increases up to about 5 cph. On the other hand, the 400 m separation record tends to oscillate more narrowly around zero. This suggests a tendency for much higher variability for horizontal scales of the order of 100 m, but less than 400 m. Furthermore, the general increase in phase with frequency (noted for $L = 100$ m) suggests a Doppler effect where, for a constant advection velocity, the frequency of encounter at a point produces a
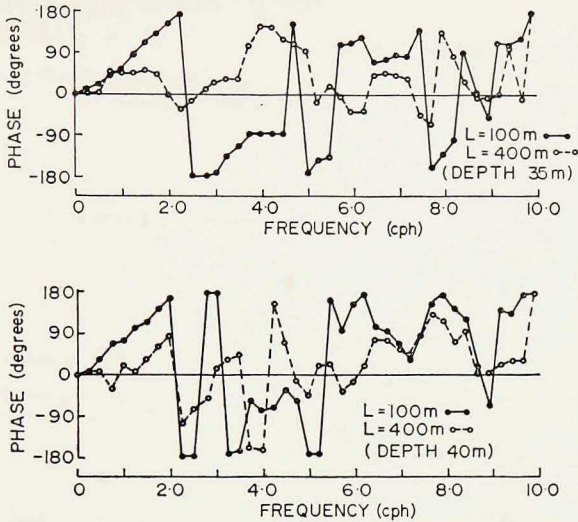
Figure 10. Phase estimated for 35 and 40 m depths.

phase shift which would increase linearly with frequency (or in the case of a frozen pattern—wave number).

Beyond 0.5 cph, a curious high correlation of the curve occurs. The significance of this is unclear, however, because beyond 4-5 cph the coherence (Fig. 9) becomes insignificant. As with the coherences, the overall similarities do suggest the high stability of the statistics.

There is a discrepancy in the values for the L = 100 m curves (Fig. 9), which could be related to the decrease in temperature gradient (i.e., density) from 35-40 m. To examine coherence variability with depth, coherence estimates for all sensor pairs for the L = 100 and 400 m separations were contoured to provide a map of iso-coherence lines with depths (Figs. 11 A, 11 B). The $f^{1/2}$ line is emphasized, and for clarity the coherence below 0.40 is omitted.

It was previously noted that the mean temperature gradients (Fig. 4B) are essentially identical to the buoyancy frequencies, and as such indicate that because of increased winds during the L = 400 m experiment, structure between 0-10 m was altered; the deeper thermal structure, however, appears unaffected. Thus, below 10 m this allows us to make a more meaningful intercomparison of the statistics at the two separations.

The coherence diagrams indicate:

(1) For L = 100 m coherence is strongly depth-dependent, peaking out at 30 m corresponding to a region of maximum temperature (density) gradient (Fig. 4B). For L = 400 m coherence below 10 m is much less depth-dependent and has lower values than for the L = 100 m separation.

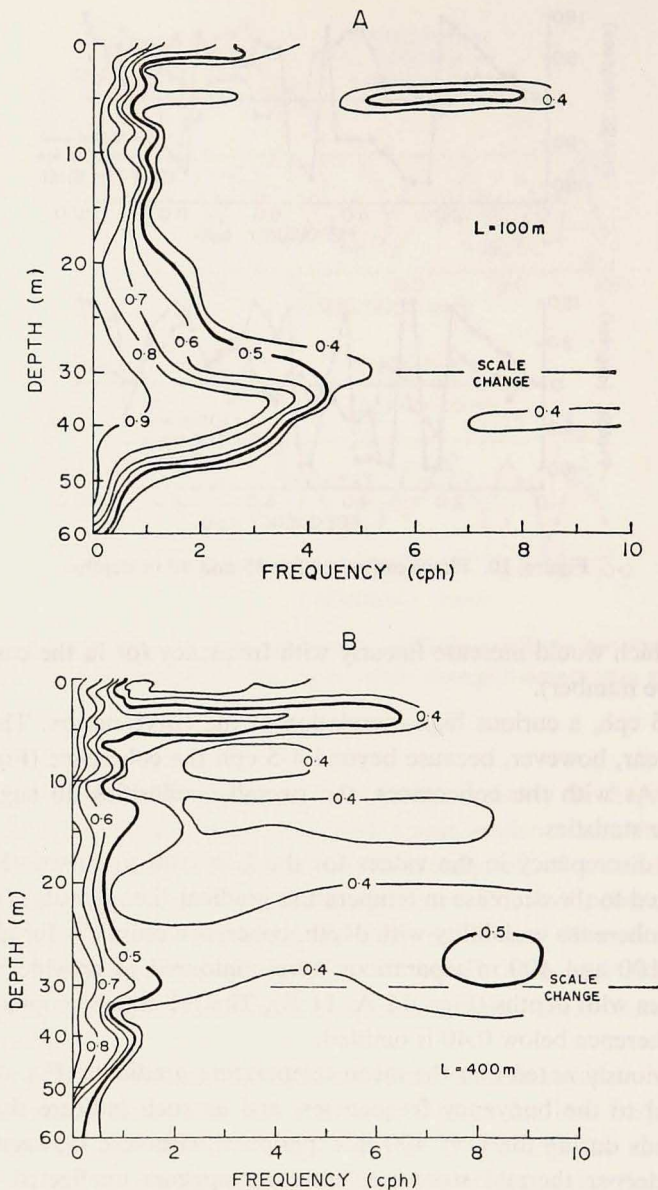Figure 11. Cross-spectral coherence contoured with depth from statistics of each record, A (L = 100 m) and B (= 400 m).

(2) Above 10 m strong depth dependence occurs with maximum coherence extension of high frequencies at about 5 m; this is more pronounced at $L = 400$ m. In contrast to the deeper coherences, this effect is probably associated with the deepening of upper mixed layer during the high winds.

Table 1. The ratios of spectral densities $(°C)^2/cph$ at a frequency of 1.0 cph, to that of 0.1 cph at various depths.

Sensor Depth (m)	Energy Ratio (%)
1	0.04
5	2.9
10	17.0
35	1.4
60	4.6

6. Discussion

Garrett and Munk (1972) and Briscoe (1975) suggest relationships wherein $f^{1/2}$ varies inversely with horizontal separation of sensors and is independent of buoyancy frequency. The Garrett and Munk model and Briscoe's data, however, pertain to the deeper ocean, a regime of relatively uniform and small buoyancy frequency. Our observed strong depth dependence at the surface layer may partly derive from the variability due to horizontal advection of random fluctuations, the intensity or amplitude of which are themselves very depth-dependent. This variability is indicated by Figure 4A, which shows the mean horizontal variability (i.e., temperature differences) correlating highly with the coherence (Fig. 11A, 11B) both at 100 and 400 m separations.

The coherence maximums in the 3-6 m depth range indicated that up to 6-9 cph fluctuations in the strong gradients possessed horizontal scales of the order of the spacing of the buoys or larger. Pinkel (1975) estimates horizontal coherences from temperature isotherm slope data obtained from booms 30 m apart on the FLIP platform. These dimensions were apparently small relative to internal wave scales present, since he obtained high coherences over a broad frequency band, analogous to our high values for L = 100 m. According to Pinkel, if coherence tends to increase (instead of the usual decrease) with frequency (and ours does between 4 and 7 cph at 3-5 m), this indicates that the lower modes tend to dominate.

The question still remains as to the major cause of temperature variability other than the surface heating as displayed by Fig. 3; is it horizontal advection of large and variable temperature gradients, or vertical oscillations of isotherms associated with internal waves or both? Returning to the auto-spectra (Fig. 8), clearly most of the contribution to the variance of the temperature signals is at frequencies below 1 cph. This fact is delineated by Table 1, which shows the proponderance of spectral density at 0.1 cph relative to that at 1.0 cph. Except at 10 m, the energy content of fluctuations at frequencies above 1 cph is negligible. The first mode internal wave calculation shows that typical phase speeds for wave frequencies less than 1 cph are roughly 100 cm/sec or greater. These high phase velocities of the low frequency internal waves suggest small phase lags between buoy records. However, from Fig. 10 the phase lags increase rapidly with frequency (at L = 100 m) almost linearly

with a slope of about $\pi/2$ cph or 15 minutes. These large phase lags suggest that low mode internal waves (which appear to dominate) have relatively low energy (amplitude). This reasoning, coupled with the observation that observed gross temperature variability appears to move through the array with the current speeds similar to those measured, indicates that much of observed temperature variability at the two buoys is advective in nature.

7. Conclusions

From our use of the COBLAMED satellite buoy pair to study horizontal variability of temperature structure in and above the late summer Mediterranean thermocline, the following conclusions are presented:

A. Analysis of the raw temperature data, together with the statistical results of consistent time lags of certain thermal events, general high correlation between records, the linear cross spectral coherence phase increase at lower frequencies and vanishing auto-spectral energy above 1 cph suggest the following picture: The 60 m thick layer has surface perturbations of diurnal heating and variable wind mixing. Both of these effects tend to smooth out the ambient variability in the upper 3-8 m depending upon their intensities. The ambient variability within the water column is in fact composed of two basic phenomena;

(1) Mesoscale (say 0.5-5 km) quasi randomly distributed patches of warm or cold water which are advected as "frozen turbulence" with the local mean current ($\sim$ 20 cm/sec) and

(2) Lower mode internal waves, most of which have frequencies < 1 cph and wave lengths much greater than 100-400 m (the buoy separations), and which propagate faster than the advection speeds.

B. Values for horizontal cross-spectral coherence $f^{1/2}$ were generally large from 0.1 to 4.5 cph. Coherences were 2.4 times greater for the 100 m separation than for 400 m and in general horizontal coherences were quite depth-variable with the $f^{1/2}$ function appearing to vary as the buoyancy frequency.

C. The use of one or more satellite buoys with oceanographic sensors, tethered and remaining down current from a taut moored buoy, appears to be a viable means of studying spatial fluctuations whereby wavelike phenomena and advected events such as moving thermal fronts, eddies and smaller scale "patchiness" are readily measured. The method should be especially effective where there is a pronounced mean flow whose scales of lateral variability (meandering) are larger than the buoy separations. Further, the ability to control the spatial separations would allow close scrutiny of the effects of current on Doppler shifting of internal wave spectra. "Buoys

of Opportunity" could be utilized in such larger scale experiments as GATE and MODE to obtain smaller scale information of ocean variability.

REFERENCES

Briscoe, M. G. 1975. Preliminary results from the tri-moored internal wave experiment. Jour. Geophys. Res., *80,* 3872–3884.

Garrett, C. W. J. and W. Munk. 1972. Space-time scales of internal waves. Geophys. Fluid Dynam., *2,* 225–264.

Granger, C. W. J. and M. Hatanaka. 1964. Spectral Analysis of Economic Time Series, Princeton Univ. Press. Princeton, N.J., 299 pp.

Kinsman, B. 1965. Wind Waves, Their Generation and Propagation on The Ocean Surface. Prentice-Hall, Englewood Cliffs, N.J., 676 pp.

Mollo-Christensen, Erik. 1970. The collection of facts needed for an adequate understanding of air-sea interaction and other flux processes, *in* A Century of Weather Progress. Am. Meteor. Soc.

Pinkel, R. 1975. Upper ocean internal wave observations from FLIP. J. Geophys. Res., *80,* 3892–3910.

Schott, F. 1971. On horizontal coherence and internal wave propagation in the North Sea. Deep Sea Res., *18,* 201–307.

Shonting, D. 1974. Current observations from the western Mediterranean during COBLAMED '69, Limnol. Oceanogr. *19,* 866–874.

—— 1969. Rhode Island Sound square kilometer study 1969; Flow patterns and kinetic energy distribution. J. Geophys. Res., *74,* 3386–3395.

Shonting, D. and L. Goodman. 1978. Temperature variability and wind mixing observed in the western Mediterranean during COBLAMED '69. J. Phys. Oceanogr. (submitted for publication). ·

Shonting, D., J. Ziengenbein, R. Pesaresi, A. DeHaen, F. de Strobel, R. Dellamaggiora. 1972. The SACLANTCEN temperature profiling system, Ocean '72. Inst. Elec. & Electron Eng. Conf. (1972, Newport, R.I.).

Siedler, G. 1971. Vertical coherence of short periodic current variations. Deep Sea Research, *18,* 179–191.

Webster, T. F. 1972. Estimates of the coherence of ocean currents over vertical distances. Deep Sea Research, *19,* 35–44.

—— 1968. Vertical profiles of horizontal ocean currents. Deep Sea Res., *16,* 85–98.

Zalkan, R. L. 1970. High frequency internal waves in the Pacific Ocean. Deep Sea Res., *17,* 91–108.